FEBS Open Bio 4 (2014) 229–239

FEBS openbio

journal homepage: www.elsevier.com/locate/febsopenbio

Ursolic acid, a natural pentacyclic triterpenoid, inhibits intracellular trafficking of proteins and induces accumulation of intercellular adhesion molecule-1 linked to high-mannose-type glycans in the endoplasmic reticulum

Satoshi Mitsuda, Tomonobu Yokomichi, Junpei Yokoigawa, Takao Kataoka *

Department of Applied Biology, Kyoto Institute of Technology, Matsugasaki, Sakyo-ku, Kyoto 606-8585, Japan

ARTICLE INFO

Article history:
Received 3 February 2014
Revised 10 February 2014
Accepted 19 February 2014

Keywords:
Glycosylation
Golgi apparatus
Intercellular adhesion molecule-1
Intracellular trafficking
Ursolic acid

ABSTRACT

Ursolic acid (3β-hydroxy-urs-12-en-28-oic acid) is a natural pentacyclic triterpenoid that is present in many plants, including medicinal herbs, and foods. Ursolic acid was initially identified as an inhibitor of the expression of intercellular adhesion molecule-1 (ICAM-1) in response to interleukin-1α (IL-1α). We report here a novel biological activity: ursolic acid inhibits intracellular trafficking of proteins. Ursolic acid markedly inhibited the IL-1α-induced cell-surface ICAM-1 expression in human cancer cell lines and human umbilical vein endothelial cells. By contrast, ursolic acid exerted weak inhibitory effects on the IL-1α-induced ICAM-1 expression at the protein level. Surprisingly, we found that ursolic acid decreased the apparent molecular weight of ICAM-1 and altered the structures of N-linked oligosaccharides bound to ICAM-1. Ursolic acid induced the accumulation of ICAM-1 in the endoplasmic reticulum, which was linked mainly to high-mannose-type glycans. Moreover, in ursolic-acid-treated cells, the Golgi apparatus was fragmented into pieces and distributed over the cells. Thus, our results reveal that ursolic acid inhibits intracellular trafficking of proteins and induces the accumulation of ICAM-1 linked to high-mannose-type glycans in the endoplasmic reticulum.

1. Introduction

Pro-inflammatory cytokines, such as interleukin-1 (IL-1), induce the expression of a variety of genes essential for inflammatory responses, including intercellular adhesion molecule-1 (ICAM-1; CD54) [1,2]. ICAM-1 is a transmembrane glycoprotein consisting of 505 amino acids and possesses multiple N-linked glycosylation sites [3,4]. ICAM-1 interacts with β2 integrins LFA-1 (CD11a/CD18) and Mac-1 (CD11b/CD18) expressed on the surface of leukocytes [5,6]. Upon stimulation with pro-inflammatory cytokines, vascular endothelial cells are induced to express cell-surface ICAM-1, which mediates the interaction with circulating leukocytes and is necessary for their tissue infiltration [7]. The level of ICAM-1 expression on the cell-surface is mainly regulated at the step of transcription. The transcription factor nuclear factor κB (NF-κB) plays a major role in the induction of ICAM-1 expression [8,9].

Pro-inflammatory cytokines, such as IL-1, induce the NF-κB signaling pathway, which is involved in not only inflammatory disease, but also cancer and metabolic disease [10,11]. The inhibitor of NF-κB (IκB) family of proteins forms a complex with the NF-κB heterodimer in the cytosol [12,13]. In response to IL-1α or IL-1β, IL-1 receptor mainly induces the activation of IκB kinase that phosphorylates IκB at the N-terminal serine residues, and phosphorylated IκB is immediately ubiquitinated and hydrolyzed by the proteasome [14,15]. The NF-κB heterodimer becomes free and translocates to the nucleus where it promotes the transcription of many target genes by binding to their κB sites [16]. It has been reported that various types of small molecules inhibit the NF-κB signaling pathway and the NF-κB-dependent gene expression [17,18].

Abbreviations: BSA, bovine serum albumin; Endo H, endoglycosidase H; ER, endoplasmic reticulum; HRP, horseradish peroxidase; HUVEC, human umbilical vein endothelial cells; ICAM-1, intercellular adhesion molecule-1; IκB, inhibitor of nuclear factor κB; IL-1, interleukin-1; MTT, 3-(4,5-dimethylthiazol-2-yl)-2,5-diphenyltetrazolium bromide; NF-κB, nuclear factor κB; PBS, phosphate-buffered saline; PNGase F, peptide: N-glycosidase F

* Corresponding author. Tel./fax: +81 75 724 7752.
E-mail address: takao.kataoka@kit.ac.jp (T. Kataoka).

http://dx.doi.org/10.1016/j.fob.2014.02.009
2211-5463/

Ursolic acid (3β-hydroxy-urs-12-en-28-oic acid), a natural pentacyclic triterpenoid carboxylic acid, is found as a major constituent in many plants, including medicinal herbs and edible plants. It has been shown that ursolic acid exerts a wide range of biological activities, including anti-inflammatory activity [19,20]. We previously isolated ursane-, oleanane-, lupane-, and taraxasterane-type triterpenes from *Nerium oleander* and our structure–activity relationship study revealed that ursolic acid inhibits the expression of cell-surface ICAM-1 most effectively among these triterpenes [21,22]. In relation to these findings, it has been shown that ursolic acid blocks the NF-κB-dependent signaling pathway and its downstream gene expression [23–30]. In this study, we investigated the inhibitory mechanism of ursolic acid on the IL-1α-induced cell-surface ICAM-1 expression in human cancer cell lines and human normal cells. In contrast to previous reports, our results revealed the novel biological activity of ursolic acid targeting the intracellular trafficking of proteins.

2. Materials and methods

2.1. Cells

Human lung carcinoma A549 cells (JCRB0076) were provided by National Institute of Biomedical Innovation JCRB Cell Bank (Osaka, Japan). A549 cells and human breast adenocarcinoma MCF-7 cells were maintained in RPMI 1640 medium (Invitrogen, Carlsbad, CA, USA) supplemented with 10% heat-inactivated fetal calf serum (Nichirei Biosciences, Tokyo, Japan) and penicillin–streptomycin mixed solution (Nacalai Tesque, Kyoto, Japan). HUVEC were obtained from Lonza (Walkersville, MD, USA). HUVEC were maintained in EGM™-2 BulletKit™ (2% FBS) according to the manufacturer's protocol.

2.2. Reagents

Ursolic acid was purchased from Sigma–Aldrich (St. Louis, MO, USA). Castanospermine, concanamycin A, and tunicamycin were obtained from Wako Pure Chemical Industries (Osaka, Japan). (+)-Brefeldin A (Merck Millipore, Darmstadt, Germany), 1-deoxymannojirimycin hydrochloride (Enzo Life Sciences, Plymouth Meeting, PA, USA; Santa Cruz Biotechnology, Santa Cruz, CA, USA), 1-deoxynojirimycin hydrochloride (Cayman Chemical, Ann Arbor, MI, USA), MG-132 (Peptide Institute, Osaka, Japan) and swainsonine (Cayman) were commercially obtained.

2.3. Antibodies

Antibodies to β-actin (AC-15; Sigma–Aldrich), calnexin (EPR3632; Epitomics, Burlingame, CA, USA), E-selectin (H-300; Santa Cruz Biotechnology), glyceraldehyde-3-phosphate dehydrogenase (GAPDH) (6C5; Santa Cruz Biotechnology), Golgi matrix protein (GM130) (EP892Y; Epitomics), ICAM-1 (clone 15.2; Leinco Technologies, St. Louis, MO, USA), ICAM-1 (Clone 28; BD Biosciences, San Diego, CA, USA), NF-κB p50 (H-119; Santa Cruz Biotechnology), NF-κB p65 (C-20; Santa Cruz Biotechnology), poly(ADP-ribose) polymerase (PARP) (C-2–10; Sigma–Aldrich) and VCAM-1 (H-276; Santa Cruz) were commercially obtained.

2.4. Cell-ELISA assay

Cells were washed twice with phosphate-buffered saline (PBS) and fixed with PBS containing 1% paraformaldehyde for 15 min. The fixed cells were washed twice with PBS and blocked with PBS containing 1% bovine serum albumin (BSA) overnight. The cells were treated with anti-ICAM-1 antibody (clone 15.2) in 1% BSA–PBS for 60 min and washed three times with 0.02% Tween 20–PBS. Then, the cells were incubated with horseradish peroxidase (HRP)-conjugated antibody (Jackson ImmunoResearch, West Grove, PA, USA) in 1% BSA–PBS for 60 min and washed three times with 0.02% Tween 20–PBS. HRP activity was determined by incubation with 200 mM sodium citrate (pH 5.3) containing *o*-phenylenediamine dihydrochloride and 0.02% H_2O_2 until a yellow color developed. Absorbance at 415 nm was measured with a Model 680 microplate reader (Bio-Rad Laboratories, Hercules, CA, USA). The IL-1α-stimulated cells without test samples and no cells were used for positive control and background, respectively. ICAM-1 expression (%) was calculated by the following formula: (test samples – background)/(positive control – background) × 100.

2.5. Assay for cell viability

Cells were incubated with 3-(4,5-dimethylthiazol-2-yl)-2,5-diphenyltetrazolium bromide (MTT) at the final concentration of 500 μg/ml for 2 h. The cells were solubilized with 5% sodium dodecyl sulfate overnight. Absorbance at 595 nm was measured with the Model 680 microplate reader.

2.6. Western blotting

Cells were washed once with PBS and lysed with Triton X-100 lysis buffer (50 mM Tris–HCl (pH 7.4), 1% Triton X-100, 2 mM dithiothreitol, 2 mM sodium orthovanadate) containing the protease inhibitor cocktail Complete™ (Roche Diagnostics, Mannheim, Germany). Cell lysates as cytoplasmic fractions were collected as supernatants by centrifugation (15,300*g*, 5 min). Precipitates were washed twice with Triton X-100 lysis buffer, and then solubilized as nuclear fractions. Proteins (30 μg/lane) were separated by SDS–polyacrylamide gel electrophoresis and transferred onto Hybond-ECL nitrocellulose membranes (GE Healthcare, Piscataway, NJ, USA). The membranes were blocked with 4% skim milk in 0.5% Tween 20–PBS, and then reacted with primary antibodies and HRP-conjugated secondary antibodies (Jackson ImmunoResearch). Protein bands were developed with Western blotting detection reagent (GE Healthcare) and detected by exposure to Hyperfilm™ ECL (GE Healthcare) or ImageQuant LAS 4000 mini (GE Healthcare).

2.7. Assay for glycosidase digestion

Peptide: N-glycosidase F (PNGase F) and endoglycosidase H (Endo H) were obtained from New England Biolabs (Ipswich, MA, USA). Cell lysates were prepared as described above. Cell lysates (20 μg protein) were heated at 100 °C for 10 min and then incubated with or without PNGase F (250 units) or Endo H (250 units) at 37 °C for 60 min according to the manufacturers' protocols. Proteins were separated by SDS–polyacrylamide gel electrophoresis and analyzed by Western blotting.

2.8. Fluorescent microscopy

Coverslips were treated with Cellmatrix® Type I-C (Nitta Gelatin, Osaka, Japan) for collagen coating. Cells were cultured on the collagen-coated coverslips overnight prior to experiments. For fixation, the cells were treated with 4% paraformaldehyde–PBS for 15 min, washed three times with PBS, and then washed twice with 25 mM glycine–PBS. The cells were treated with cold methanol and washed three times with 0.3% Triton X-100–PBS for permeabilization. The fixed cells were blocked with 5% BSA–PBS overnight. The cells were stained serially with 5% BSA–PBS containing rabbit anti-GM130 antibody, rabbit anti-calnexin antibody, or mouse anti-ICAM-1 antibody for primary antibodies

and Alexa-594-conjugated anti-rabbit IgG antibody (Invitrogen) or Alexa-488-conjugated anti-mouse IgG antibody (Invitrogen) for secondary antibodies for 1 h. Then, the cells were washed three times with 0.3% Triton X-100–PBS between antigen–antibody reactions. The coverslips were mounted on glass slides with FluorSave™ (Merck Millipore). The stained cells were observed with a confocal laser scanning microscope system FV10i (Olympus, Tokyo, Japan). To quantify the morphological changes of the Golgi apparatus, cells were stained with rabbit anti-GM130 antibody and Alexa-594-conjugated anti-rabbit IgG antibody. The shapes of the Golgi apparatus were classified into a normal type (gathered in a small area), a disrupted type (fragmented and scattered over the cells) and other ambiguous types. The number of cells that harbored these particular types of the Golgi apparatus was counted over multiple fields under a fluorescence light microscope (Axiovert 200 M, Carl Zeiss, Jena, Germany) until the total cell number was more than a hundred cells.

2.9. Assay for α-mannosidase activity

α-Mannosidase from *Canavalia ensiformis* (Jack bean) (29 units/mg) and 4-nitrophenyl-α-D-mannopyranoside were obtained from Sigma–Aldrich and Tokyo Chemical Industry (Tokyo, Japan), respectively. Jack bean α-mannosidase (0.05 unit) was incubated with 50 mM sodium phosphate buffer (pH 6.8) containing 2 mM 4-nitrophenyl-α-D-mannopyranoside at 37 °C for 15 min. Absorbance at 405 nm was measured with the Model 680 microplate reader.

2.10. Statistical analysis

Statistical significance was assessed by one-way ANOVA followed by the Tukey test for multiple comparisons. Differences of $P < 0.05$ were considered to be statistically significant.

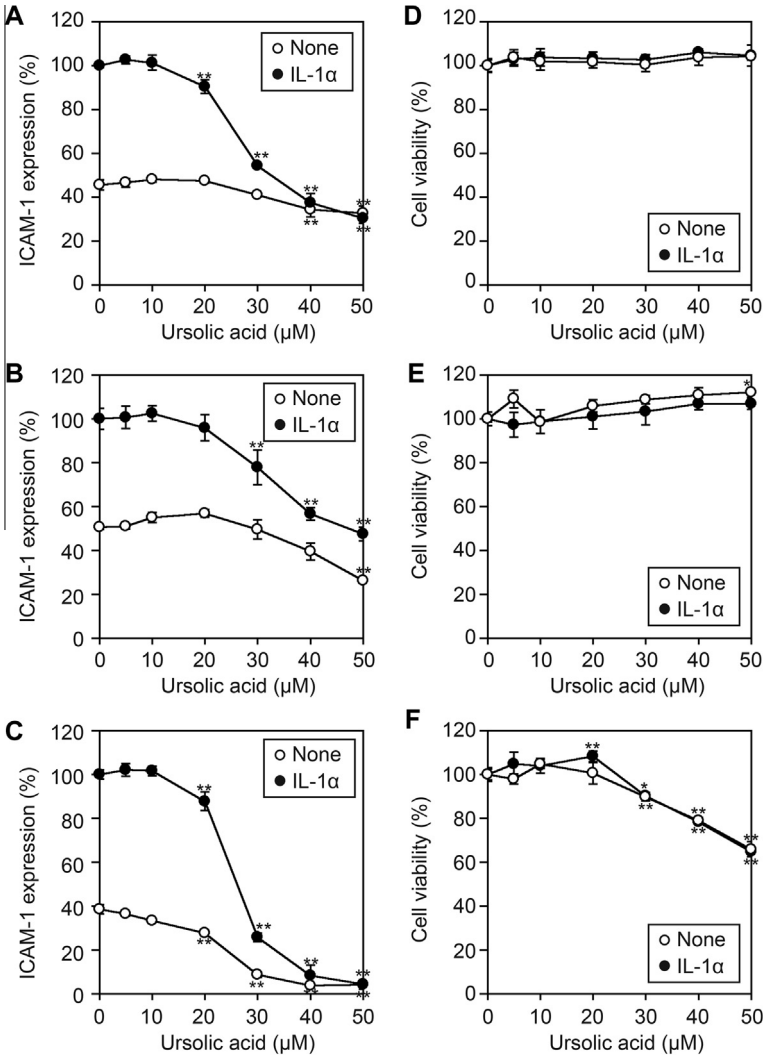

Fig. 1. Ursolic acid inhibits IL-1α-induced cell-surface ICAM-1 expression. (A–C) A549 cells (A), MCF-7 cells (B), and HUVEC (C) were preincubated with various concentrations of ursolic acid for 1 h and then incubated with (filled circles) or without (open circles) IL-1α (0.25 ng/ml) for 6 h. Cell-surface ICAM-1 expression was measured by the Cell-ELISA assay. ICAM-1 expression (%) is represented by the means ± S.D. of triplicate cultures. $^{**}P < 0.01$, compared with control. Data are representative of at least three independent experiments. (D–F) A549 cells (D), MCF-7 cells (E), and HUVEC (F) were preincubated with various concentrations of ursolic acid for 1 h and then incubated with (filled circles) or without (open circles) IL-1α (0.25 ng/ml) for 6 h. Cell viability (%) was measured by the MTT assay. Cell viability is represented by the means ± S.D. of triplicate cultures. $^{*}P < 0.05$ and $^{**}P < 0.01$, compared with control. Data are representative of three independent experiments.

3. Results

3.1. Ursolic acid inhibits IL-1α-induced cell-surface ICAM-1 expression

Human lung carcinoma A549 cells and human breast adenocarcinoma MCF-7 cells were induced to express ICAM-1 in response to IL-1α stimulation [31,32]. A549 cells and MCF-7 cells were preincubated with ursolic acid for 1 h and then incubated with IL-1α for 6 h. Then, the amount of cell-surface ICAM-1 was quantitated by the Cell-ELISA assay. Ursolic acid inhibited the IL-1α-induced cell-surface ICAM-1 expression in A549 cells in a dose-dependent manner and almost completely at concentrations higher than 30 μM (Fig. 1A). The IL-1α-induced cell-surface ICAM-1 expression in MCF-7 cells was also inhibited by ursolic acid (Fig. 1B). In addition to those cell lines, HUVEC were induced to express cell-surface ICAM-1 in response to IL-1α. Ursolic acid at concentrations higher than 30 μM inhibited the IL-1α-induced cell-surface ICAM-1 expression in HUVEC (Fig. 1C). In A549 cells and MCF-7 cells, ursolic acid did not affect cell viability even at concentrations as high as 50 μM (Fig. 1D and E). In HUVEC, ursolic acid decreased cell viability partially at concentrations that inhibited ICAM-1 expression (Fig. 1F). However, it seems that ursolic acid can exert cytotoxic effects over longer time periods, since ursolic acid decreased cell viability during 24 h incubation in A549 cells (Fig. S1). Together, these data indicate that ursolic acid inhibits the expression of cell-surface ICAM-1 induced by IL-1α in human cancer cells and normal cells.

3.2. Ursolic acid affects IL-1α-induced ICAM-1 post-translational modification

We next investigated the effect of ursolic acid on the NF-κB signaling pathway induced by IL-1 receptor. Ursolic acid slightly augmented the IL-1α-induced translocation of NF-κB subunits, p65 and p50, from the cytoplasm to the nucleus in A549 cells (Fig. S2). These data suggested that ursolic acid inhibits cell-surface ICAM-1 expression at the steps downstream of NF-κB activation. We therefore examine the effect of ursolic acid on ICAM-1 expression at the protein level by Western blotting. ICAM-1 was detected as multiple bands migrating to more than 80 kDa in A549 cells stimulated with IL-1α (Fig. 2A). Unexpectedly, we found that ursolic acid weakly affected the total amount of ICAM-1 but decreased the molecular weight of ICAM-1 to 60–70 kDa in A549 cells (Fig. 2A). In MCF-7 cells and normal human umbilical vein endothelial cells (HUVEC), ursolic acid also decreased the molecular weight of ICAM-1 to values similar to those observed in A549 cells (Fig. 2B and C). In addition, ursolic acid decreased the molecular weights of E-selectin and VCAM-1 in HUVEC (Fig. 2C). These results indicate that ursolic acid marginally reduces the IL-1α-induced protein synthesis of ICAM-1 but affects the post-translational modification of ICAM-1.

3.3. Ursolic acid affects N-linked oligosaccharide processing of ICAM-1

ICAM-1 is a transmembrane glycoprotein consisting of 505 amino acids and possesses multiple consensus sites for N-linked glycosylation [3,4]. Tunicamycin is known to block the synthesis of N-linked oligosaccharides on glycoproteins [33]. Consistent with a previous report [34], an unglycosylated form of ICAM-1 was detected as bands migrating to around 50–55 kDa in tunicamycin-treated cells (Fig. 3A). Indeed, the size of ICAM-1 in the tunicamycin-treated cells was apparently smaller than that in the ursolic-acid-treated cells (Figs. 2A, 3A). Moreover, tunicamycin at concentrations higher than 1 μM decreased the cell-surface ICAM-1 expression in A549 cells (Fig. 3B). By contrast, tunicamycin did not affect cell viability at concentrations up to 10 μM during 6 h incubation (Fig. 3C).

Glycoproteins undergo N-linked oligosaccharide processing during intracellular trafficking. Cell lysates were subjected to PNGase F or Endo H digestion and Western blot analysis. ICAM-1 was converted by PNGase F into an unglycosylated form migrating at 50–55 kDa (Fig. 3D). Endo H was unable to digest ICAM-1 in untreated A549 cells (Fig. 3D). By contrast, Endo H was able to digest the oligosaccharide chains of ICAM-1 in ursolic-acid-treated A549 cells (Fig. 3D). Thus, these data indicate that high-mannose-type glycans are mainly linked to ICAM-1 in ursolic-acid-treated cells.

3.4. Ursolic acid induces accumulation of ICAM-1 in endoplasmic reticulum (ER)

The subcellular localization of ICAM-1 was further analyzed by confocal microscopy (Figs. S3 and S4 for lower magnification images, and Fig. 4A and B for higher magnification images of rep-

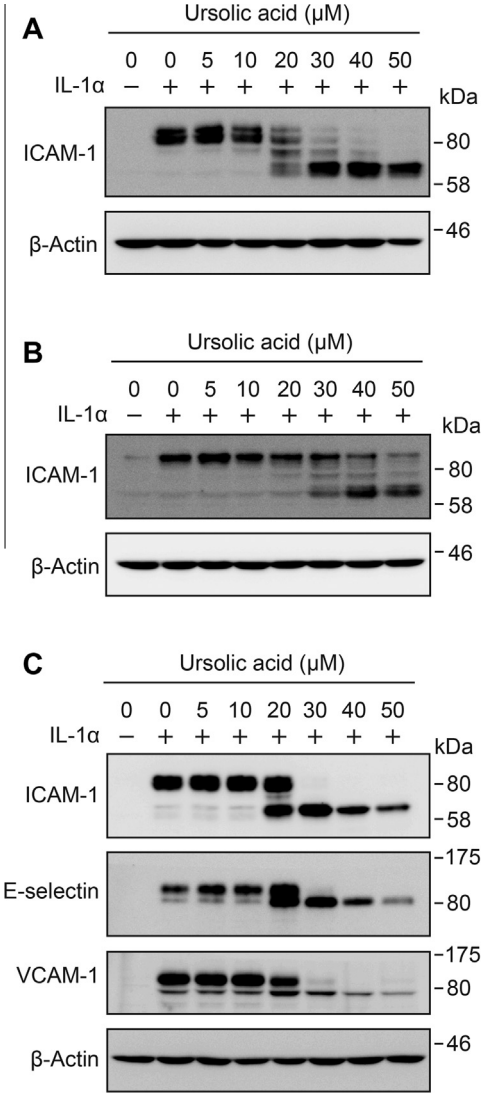

Fig. 2. Ursolic acid does not inhibit IL-1α-induced expression of ICAM-1 at the protein level but affects its post-translational modification. A549 cells (A), MCF-7 cells (B), and HUVEC (C) were preincubated with various concentrations of ursolic acid for 1 h and then incubated with IL-1α (0.25 ng/ml) for 6 h. Cell lysates were analyzed by Western blotting. Data are representative of at least three independent experiments for A549 cells and MCF-7 cells and two independent experiments for HUVEC.

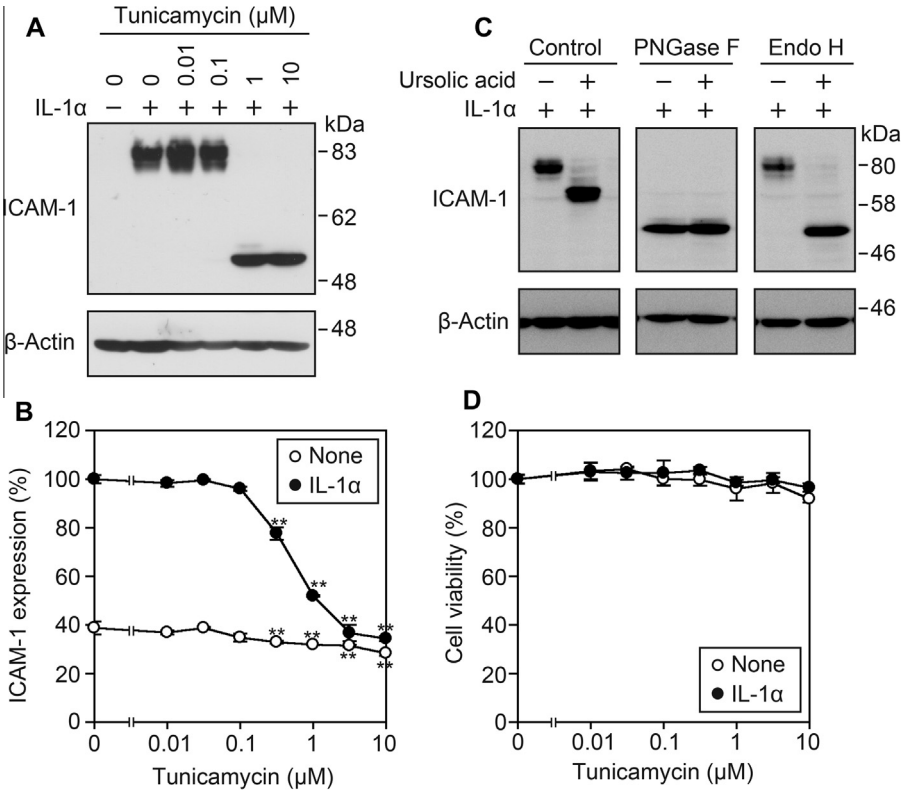

Fig. 3. Ursolic acid affects N-linked oligosaccharide processing of ICAM-1. (A) A549 cells were treated with various concentrations of tunicamycin for 1 h and then incubated with (+) or without (–) IL-1α (0.25 ng/ml) for 6 h. Cell lysates were analyzed by Western blotting. Data are representative of three independent experiments. (B) A549 cells were preincubated with various concentrations of tunicamycin for 1 h and then incubated with (filled circles) or without (open circles) IL-1α (0.25 ng/ml) for 6 h. Cell-surface ICAM-1 expression was measured by the Cell-ELISA assay. ICAM-1 expression (%) is represented by the means ± S.D. of triplicate cultures. $^{**}P < 0.01$, compared with control. Data are representative of four independent experiments. (C) A549 cells were preincubated with various concentrations of tunicamycin for 1 h and then incubated with (filled circles) or without (open circles) IL-1α (0.25 ng/ml) for 6 h. Cell viability (%) was measured by the MTT assay. Cell viability (%) is represented by the means ± S.D. of triplicate cultures. Data are representative of three independent experiments. (D) A549 cells were preincubated with (+) or without (–) ursolic acid (50 μM) for 1 h and then incubated with (+) IL-1α (0.25 ng/ml) for 6 h. Cell lysates were treated or not treated with PNGase F or Endo H, and analyzed by Western blotting. Data are representative of three independent experiments.

resentative cells). GM130 and calnexin are localized in the Golgi apparatus and the ER, respectively [35,36]. Control A549 cells did not express ICAM-1, whereas IL-1α stimulation induced the expression of ICAM-1 over the whole cell including the cell periphery (Fig. 4A and B). Only a part of ICAM-1 was co-localized with GM130 and calnexin in IL-1α-stimulated cells (Fig. 4A and B). This staining pattern suggests that a large part of ICAM-1 is transported from the Golgi apparatus and present on the cell surface. When A549 cells were preincubated with ursolic acid and then incubated with IL-1α, ICAM-1 was accumulated around the nucleus and co-localized markedly with calnexin but barely with GM130 (Fig. 4A and B). Thus, these results indicate that ursolic acid induces the accumulation of ICAM-1 in the ER. In addition, we observed that the Golgi apparatus is fragmented and scattered over the cells upon exposure to ursolic acid regardless of the presence or absence of IL-1α (Fig. 4A). To quantify the morphological changes of the Golgi apparatus, the shapes of the Golgi apparatus were classified into a normal type, a disrupted type and other types by using fluorescent microscopy. Ursolic acid significantly decreased the percentage of cells harboring the normal Golgi apparatus, and conversely increased the percentage of cells harboring the disrupted Golgi apparatus (Fig. 5A and B).

3.5. Ursolic acid attenuates N-linked oligosaccharide processing of ICAM-1 at steps similar to 1-deoxymannojirimycin

A number of alkaloid-type compounds are known to inhibit N-linked glycoprotein processing [37]. Brefeldin A induces the disassembly and redistribution of the Golgi apparatus and inhibits protein transport [38,39]. To gain an insight into the mode of action of ursolic acid, we further investigated the effects of these inhibitors on ICAM-1 expression. 1-Deoxynojirimycin (an inhibitor of α-glucosidase I) at concentrations of up to 100 μM did not obviously affect the molecular weight of ICAM-1, whereas castanospermine (also an inhibitor of α-glucosidase I), swainsonine (an inhibitor of Golgi α1,2-mannosidase II), and concanamycin A (an inhibitor of vacuolar type H^+-ATPase) decreased the molecular weight of ICAM-1 to a value between those of control cells and ursolic-acid-treated cells (Fig. 6A). By contrast, brefeldin A (an inhibitor of protein transport) at the concentration of 100 nM decreased the molecular weight of ICAM-1 to a value similar to that observed in the ursolic-acid-treated cells (Fig. 6A and B). In addition to brefeldin A, 1-deoxymannojirimycin (an inhibitor of Golgi α1,2-mannosidase I) at the concentration of 100 μM decreased the molecular weight of ICAM-1 to a value similar to that observed with ursolic acid (Fig. 6A and C).

Cell lysates prepared from brefeldin-A- or 1-deoxymannojirimycin-treated A549 cells were digested with PNGase F or Endo H and analyzed by Western blotting. In the brefeldin-A-treated A549 cells, Endo H did not digest ICAM-1 to sizes similar to that observed by PNGase F digestion (Fig. 6D), indicating that ICAM-1 contains both high-mannose-type and other-type oligosaccharide chains in a single polypeptide. In the 1-deoxymannojirimycin-treated cells, ICAM-1 was sensitive to Endo H, and most of ICAM-1 was digested by Endo H into multiple fragments whose molecular weights were similar to or slightly higher than those of fragments obtained by PNGase F digestion (Fig. 6D).

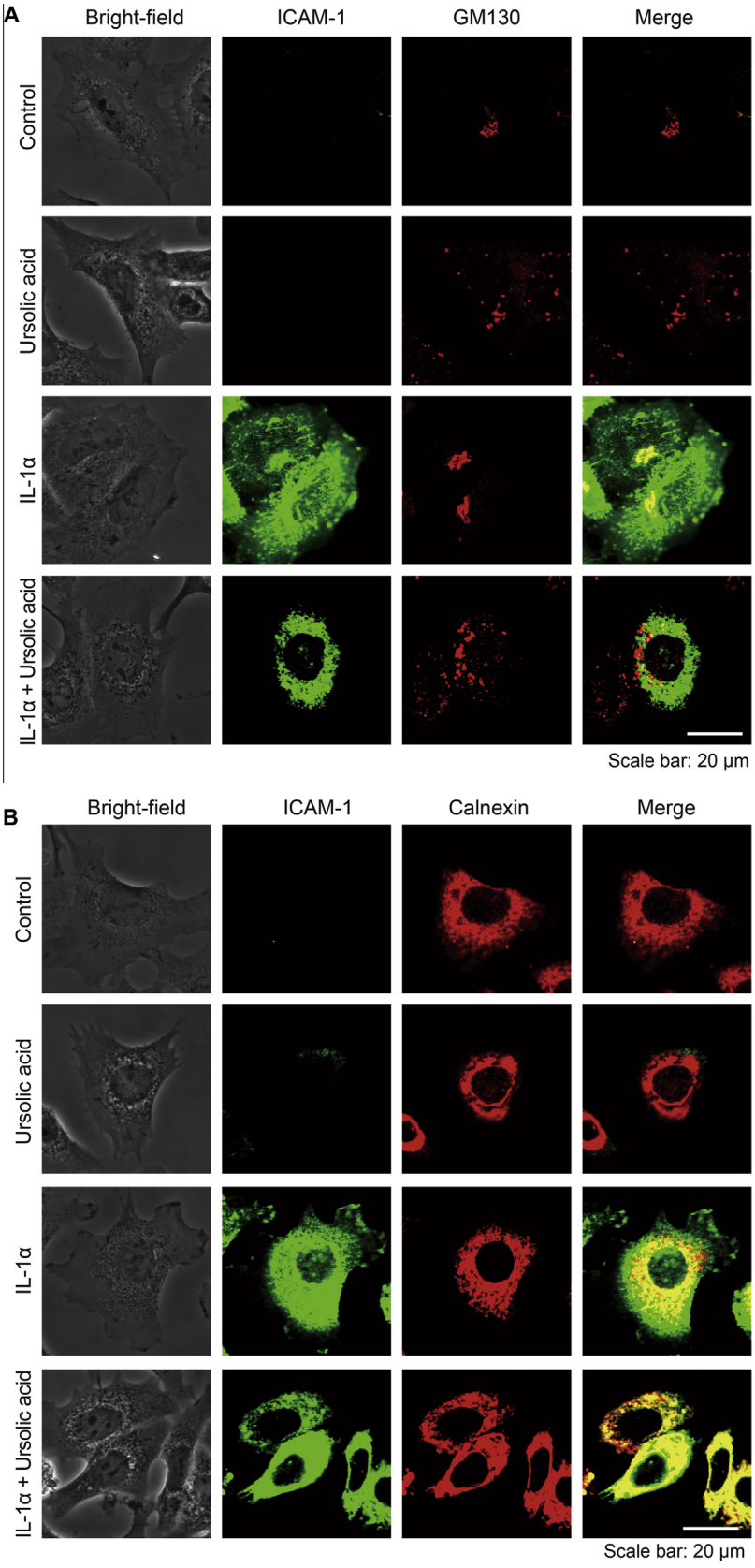

Fig. 4. Ursolic acid induces accumulation of ICAM-1 in ER. A549 cells were preincubated with or without ursolic acid (50 μM) for 1 h and then incubated with or without IL-1α (0.25 ng/ml) for 6 h in the presence or absence of ursolic acid. Cells were fixed and stained for ICAM-1 (green), together with GM130 (red) (A) and calnexin (red) (B) as markers of Golgi apparatus and ER, respectively. Panels A and B show higher magnification images of representative cells in Figs. S3 and S4, respectively. Scale bars represent 20 μm. Data are representative of at least three independent experiments. (For interpretation of the references to colour in this figure legend, the reader is referred to the web version of this article.)

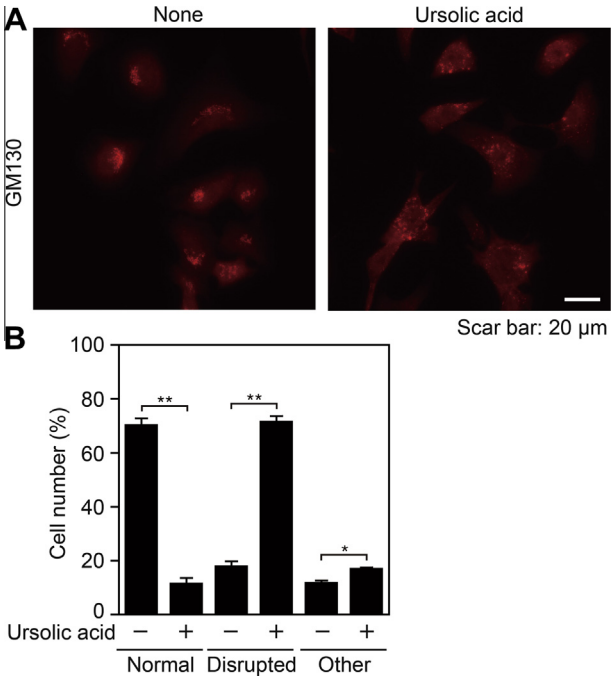

Fig. 5. Ursolic acid induces morphological changes of Golgi apparatus. A549 cells were incubated in the presence or absence of ursolic acid (50 μM) for 6 h. Cells were stained for GM130 (red), and the shapes of the Golgi apparatus were observed under a fluorescence light microscope (A). Scale bars represent 20 μm. The number of cells harboring a normal type, a disrupted type, and other types of the Golgi apparatus was measured (B). Cell number (%) is represented by the means ± S.D. of three independent experiments. (For interpretation of the references to colour in this figure legend, the reader is referred to the web version of this article.)

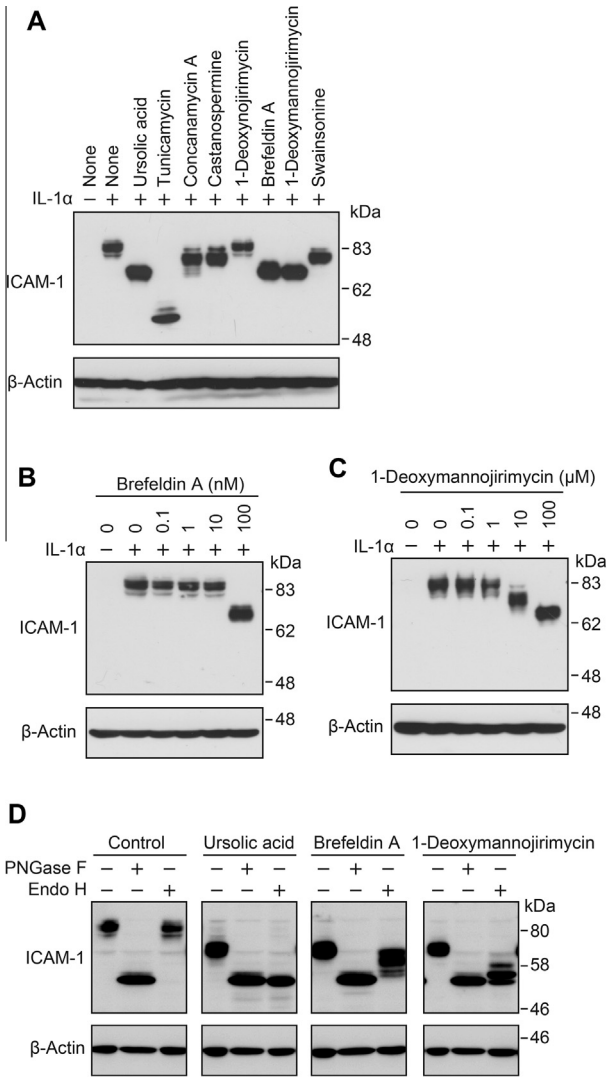

Fig. 6. Ursolic acid attenuates N-linked oligosaccharide processing in a manner similar to brefeldin A or 1-deoxymannojirimycin. (A–C) A549 cells were preincubated with or without ursolic acid (50 μM), tunicamycin (1 μM), concanamycin A (10 μM), castanospermine (300 μM), 1-deoxynojirimycin (100 μM), brefeldin A (100 nM), 1-deoxymannojirimycin (100 μM) or swainsonine (100 nM) for 1 h and incubated with (+) or without (−) IL-1α (0.25 ng/ml) for 6 h in the presence or absence of the compounds (A). A549 cells were preincubated with various concentrations of brefeldin A (B) or 1-deoxymannojirimycin (C) for 1 h and incubated with (+) or without (−) IL-1α (0.25 ng/ml) for 6 h. Cell lysates were analyzed by Western blotting. Data are representative of at least two independent experiments. (D) A549 cells were preincubated with or without ursolic acid (50 μM), brefeldin A (100 nM) or 1-deoxymannojirimycin (100 μM) for 1 h and then incubated with IL-1α (0.25 ng/ml) for 6 h. Cell lysates were treated (+) or not treated with (−) PNGase F or Endo H and analyzed by Western blotting. Data are representative of three independent experiments.

3.6. Ursolic acid inhibits intracellular trafficking from ER to Golgi apparatus in a manner distinct from brefeldin A

The IL-1α-induced cell-surface ICAM-1 expression was reduced to less than 20% by 1-deoxynojirimycin (up to 100 μM), castanospermine (up to 300 μM), and swainsonine (up to 1 μM) in A549 cells (data not shown). Moreover, 1-deoxymannojirimycin at concentrations up to 100 μM did not inhibit the IL-1α-induced cell-surface ICAM-1 expression (Fig. 7A). By contrast, brefeldin A at concentrations higher than 100 nM inhibited the IL-1α-induced cell-surface ICAM-1 expression almost completely (Fig. 7B). Thus, it seems that ICAM-1 can be efficiently transported to the cell surface without trimming by α-glucosidases or α-mannosidases. Ursolic acid barely affected the activity of Jack bean α-mannosidase (Fig. 8A), whereas 1-deoxymannojirimycin inhibited the enzyme activity (Fig. 8B).

The intracellular localization of ICAM-1 in A549 cells exposed to brefeldin A or 1-deoxymannojirimycin was further analyzed by confocal microscopy (Figs. S5 and S6 for lower magnification images, and Fig. 9A and B for higher magnification images of representative cells). Brefeldin A, but not 1-deoxymannojirimycin, was found to induce the fragmentation of the Golgi apparatus (Fig. 9A). Brefeldin A induced the accumulation of ICAM-1 primarily in the ER, as a large part of ICAM-1 was localized at the periphery of the nucleus and co-localized with calnexin in the brefeldin-A-treated A549 cells (Fig. 9B). However, in contrast to the ursolic-acid-treated cells, ICAM-1 was also merged with GM130 to some extent in the brefeldin-A-treated cells (Fig. 9A). By contrast, the localization of ICAM-1 in the 1-deoxymannojirimycin-treated cells was similar to that in control cells, as ICAM-1 was dispersed over the whole cell and a part of ICAM-1 was co-localized with both GM130 and calnexin (Fig. 9A and B). This is consistent with the observation that 1-deoxymannojirimycin did not inhibit cell-surface ICAM-1expression (Fig. 7A).

4. Discussion

Ursolic acid has been reported to possess multiple biological activities [19,20]. We previously reported that ursolic acid inhibits cell-surface ICAM-1 expression in response to inflammatory cytokines [21,29]. In line with those reports, ursolic acid has been reported to inhibit the constitutive expression of ICAM-1 in cancer cell lines and the TNF-α-induced ICAM-1 expression in HUVEC [40–43]. Moreover, we found that ursolic acid reduces the

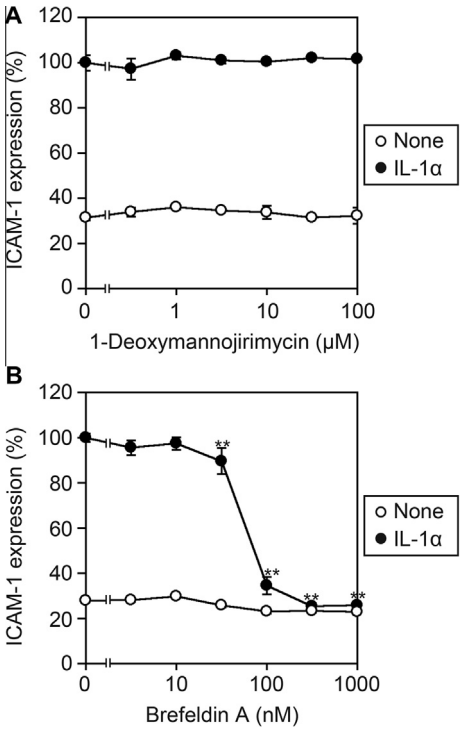

Fig. 7. Brefeldin A, but not 1-deoxymannojirimycin, inhibits IL-1α-induced cell-surface ICAM-1 expression. A549 cells were preincubated with various concentrations of 1-deoxymannojirimycin (A) or brefeldin A (B) for 1 h and then incubated with IL-1α (0.25 ng/ml) for 6 h. Cell-surface ICAM-1 expression was measured by the Cell-ELISA assay. ICAM-1 expression (%) is represented by the means ± S.D. of triplicate cultures. $^{**}P < 0.01$, compared with control. Data are representative of at least three independent experiments.

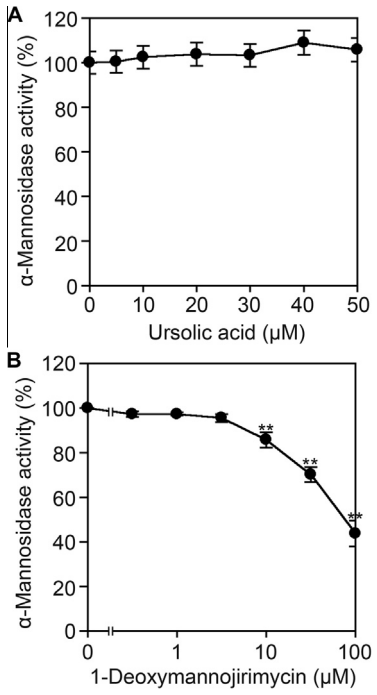

Fig. 8. Ursolic acid does not inhibit α-mannosidase activity. Jack bean α-mannosidase was preincubated with various concentrations of ursolic acid (A) or 1-deoxymannojirimycin (B) for 30 min and then incubated with 4-nitrophenyl-α-D-mannopyranoside for 15 min. α-Mannosidase activity (%) is represented by the means ± S.D. of three independent experiments.

ICAM-1 expression induced by TNF-α in part by inhibiting Na^+/K^+-ATPase and amino acid transport [29]. In contrast to those reports [29], ursolic acid exerted weak inhibitory effects on ICAM-1 expression at the protein level but profoundly inhibited cell-surface ICAM-1 expression in response to IL-1α stimulation in human cancer cell lines and normal cells. Therefore, we investigated the molecular mechanism by which ursolic acid inhibits cell-surface ICAM-1 expression. In this study, we discovered the novel biological activity of ursolic acid targeting the intracellular trafficking of proteins.

Ursolic acid inhibited the intracellular transport of glycoproteins from the ER to the Golgi apparatus. This may be ascribed to the dysfunction of the Golgi apparatus as ursolic acid induced the fragmentation of the Golgi apparatus. Brefeldin A is known to cause the disassembly of the Golgi apparatus and its redistribution to the ER [38,39]. In a manner similar to ursolic acid, the Golgi apparatus was fragmented into pieces and dispersed in brefeldin-A-treated cells. Nevertheless, ICAM-1 present in ursolic-acid-treated cells was very sensitive to Endo H, whereas ICAM-1 present in brefeldin-A-treated cells was partially resistant to Endo H. This may be due to that oligosaccharide-processing enzymes localized in the Golgi apparatus are translocated into the ER by promotion of retrograde transport and those enzymes can further modify the oligosaccharide chains in brefeldin-A-treated cells. It has been reported that ursolic acid exerts some inhibitory activity on yeast α-glucosidase [44,45]. However, specific inhibitors of α-glucosidases or α-mannosidases exerted only weak effects on the transport of ICAM-1 to the cell surface. Thus, these results suggest that ursolic acid directly targets the Golgi apparatus and thereby inhibits the intracellular trafficking of glycoproteins in a mechanism distinct from brefeldin A.

ICAM-1 possesses multiple N-linked glycosylation sites [3,4]. It has been reported that soluble ICAM-1 comprising of heavily-glycosylated N-terminal two immunoglobulin superfamily domains are mostly insensitive to Endo H when expressed in HEK293T cells [4]. Consistent with this, a large part of ICAM-1 in IL-1α-stimulated A549 cells was resistant to Endo H. By contrast, ICAM-1 present in ursolic-acid-treated cells became sensitive to Endo H. In addition, the molecular weight of ICAM-1 in the ursolic-acid-treated cells was similar to that in the 1-deoxymannojirimycin- or brefeldin-A-treated cells. We also found that ursolic acid induces the accumulation of ICAM-1 in the ER. Thus, it is most likely that the N-linked glycans of ICAM-1 in ursolic-acid-treated cells are high-mannose types prior to the digestion with Golgi α1,2-mannosidase I.

It has been recently reported that TNF-α stimulation induces the production of two distinct ICAM-1 bands in HUVEC: a major band at ~95 kDa and a minor band at ~75 kDa, which was linked to high-mannose-type glycans, and that high-mannose-type ICAM-1 is functionally distinct from fully-glycosylated ICAM-1 [46]. We observed that IL-1α induces the expression of ICAM-1 bands migrating to more than 80 kDa as major forms and those migrating to 60–70 kDa as minor forms in HUVEC. The minor ICAM-1 forms might be linked to high-mannose-type glycans, since their sizes were similar to those found in ursolic-acid-treated HUVEC. These results suggest that IL-1α itself promotes the expression of high-mannose-type ICAM-1 in a manner similar to TNF-α at least in HUVEC. However, in A549 cells, the expression of high-mannose-type ICAM-1 was barely induced by IL-1α alone. In contrast to ursolic acid that blocked the cell-surface ICAM-1 expression, 1-deoxymannojirimycin promoted the cell-surface expression of high-mannose-type ICAM-1 in IL-1α-stimulated A549 cells. Therefore, the inhibition of Golgi α1,2-mannosidase I might be one of critical steps to promote the cell-surface expression of high-mannose-type ICAM-1.

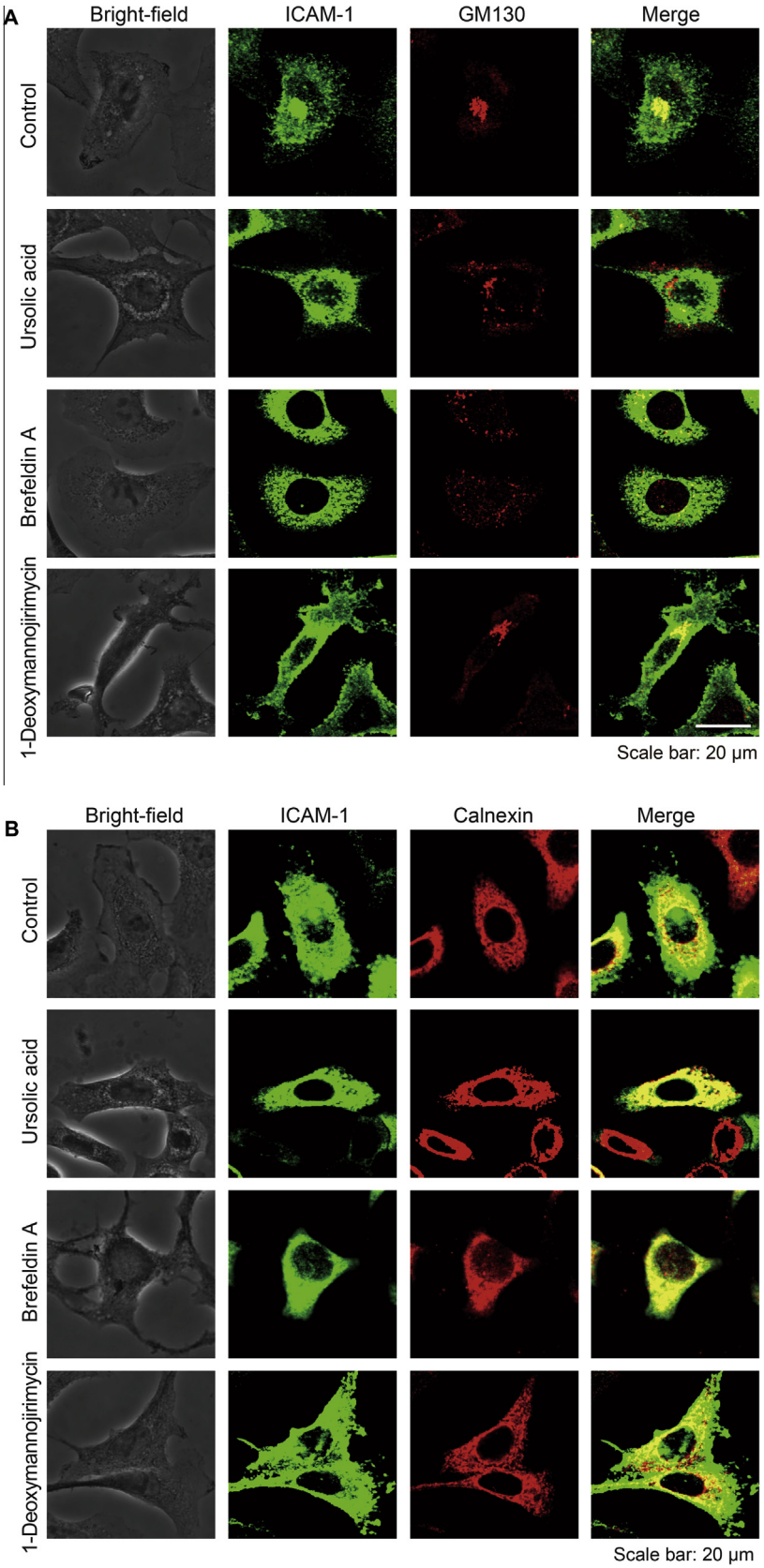

Fig. 9. Ursolic acid inhibits intracellular protein transport from ER to Golgi apparatus in a manner distinct from brefeldin A. A549 cells were preincubated with or without ursolic acid (50 μM), brefeldin A (100 nM) or 1-deoxymannojirimycin (100 μM) for 1 h and then incubated with IL-1α (0.25 ng/ml) for 6 h in the presence or absence of the compounds. Cells were fixed and stained for ICAM-1 (green), together with GM130 (red) (A) and calnexin (red) (B) as markers of Golgi apparatus and ER, respectively. Panels A and B show higher magnification images of representative cells in Figs. S5 and S6, respectively. Scale bars represent 20 μm. Data are representative of at least three independent experiments. (For interpretation of the references to colour in this figure legend, the reader is referred to the web version of this article.)

It has been shown that ursolic acid blocks the NF-κB signaling pathway activated constitutively or in response to pro-inflammatory cytokines or chemotherapeutic agents [30]. Consistent with those reports, we previously showed that ursolic acid reduces the amount of TNF-α-induced ICAM-1 mRNA by 40–50% in A549 cells [29]. Thus, this biological activity of ursolic acid contributes, at least in part, to the inhibition of the TNF-α-induced ICAM-1 expression at the protein level. In contrast to TNF-α, however, ursolic acid slightly augmented the IL-1α-induced NF-κB activation in A549 cells, and did not obviously decrease the IL-1α-induced ICAM-1 expression at the protein level in human cancer cells. By contrast, it has been reported that the IL-1β-induced NF-κB signaling pathway is inhibited by ursolic acid in rat C6 glioma cells [26]. Thus, it seems that ursolic acid blocks the IL-1-induced NF-κB signaling pathway in a cell-type-specific manner.

We previously showed that specific inhibitors of Na^+/K^+-ATPase (e.g. ouabain) block Na^+-dependent amino acid transport and thereby inhibits the NF-κB-responsive gene expression induced by TNF-α or IL-1α [47]. Ouabain did not affect the TNF-α-induced ICAM-1 mRNA expression but strongly inhibited ICAM-1 expression at the protein level [46]. We and other groups reported that ursolic acid inhibits the activity of purified Na^+/K^+-ATPase [29,48,49]. In a mechanism similar to ouabain, ursolic acid is likely to inhibit amino acid transport and *de novo* protein synthesis via the inhibition of Na^+/K^+-ATPase. However, in contrast to ouabain, ursolic acid not only decreased the TNF-α-induced expression of ICAM-1 at the protein level but also reduced the molecular weight of ICAM-1 [29]. As ouabain at any concentrations did not alter the molecular weight of ICAM-1 but solely inhibited ICAM-1 expression [47], the inhibition of Na^+/K^+-ATPase activity may not be responsible for the blockage of ICAM-1 transport to the cell surface in ursolic-acid-treated cells.

Cell-surface molecules, such as ICAM-1, are induced in response to inflammatory cytokines and play an essential role in inflammation [7]. Ursolic acid is a constituent of many plants, including medicinal herbs, and foods [19,20]. Thus, ursolic acid might be expected to a potential natural product that exhibits anti-inflammatory activity *in vivo*. To date, the pharmacokinetic studies of ursolic acid in humans and animal models have been reported [43,50–54]. The oral administration of the herb *Sambucus chinensis* L. (known as Lu-Ying) extract at a dose containing ursolic acid (80.32 mg/kg) caused the maximum concentration of 294.8 ng/ml (calculated to be 0.645 μM) in the rat plasma [50]. In mice fed orally with ursolic acid (250 mg/kg) and ursolic acid-enriched diet (1%, w/w), the serum concentrations of ursolic acid were reported to be 480 ng/ml (1.05 μM) and 600–1300 ng/ml (1.31–2.85 μM), respectively [43,51]. In humans, the oral administration of ursolic acid (32 mg) led to the concentration of 27.95 ± 14.20 ng/ml (0.061 ± 0.031 μM) [52]. Moreover, two recent studies have reported that the concentrations of ursolic acid are 3404.6 ± 748.8 ng/ml (7.45 ± 1.64 μM) and 1835–3457 ng/ml (4.02–7.57 μM) after the intravenous injection of ursolic acid in humans [53,54]. These studies suggest that the concentrations of ursolic acid are in the physiological range of ∼7.5 μM in humans. Our dose-dependent experiments have shown that ursolic acid effectively inhibits intracellular trafficking of proteins at 20–30 μM in three human cancer and normal cell lines. Thus, it seems that the physiological concentrations of ursolic acid *in vivo* are at least 4-fold lower than the concentrations reported here. The effective concentrations of ursolic acid might be optimized by *in vitro* experiments, which screen particular cell types more sensitive to ursolic acid and extend preincubation times with ursolic acid. Furthermore, *in vivo* experiments to explore the effect of ursolic acid on ICAM-1 expression and intracellular trafficking of proteins are necessary for the development of ursolic acid as an anti-inflammatory agent.

In conclusion, we found that ursolic acid affects the morphology of the Golgi apparatus and inhibits the intracellular trafficking of proteins from the ER to the Golgi apparatus. However, the biological activity of ursolic acid on the glycoprotein transport is distinct from that of brefeldin A. In this regard, ursolic acid may be a useful bioprobe for investigating the molecular mechanism underlying the intracellular trafficking of proteins and the morphology of the Golgi apparatus.

Acknowledgements

We thank Iyo Matsuda and Yuji Okina for technical assistance. This work was supported by Grants-in-Aid for Scientific Research (KAKENHI) Grant Numbers 22380060 and 25292061 (to T.K.) from the Japan Society for the Promotion of Science (JSPS).

Appendix A. Supplementary data

Supplementary data associated with this article can be found, in the online version, at http://dx.doi.org/10.1016/j.fob.2014.02.009.

References

[1] Collins, T., Read, M.A., Neish, A.S., Whitley, M.Z., Thanos, D. and Maniatis, T. (1995) Transcriptional regulation of endothelial cell adhesion molecules: NF-κB and cytokine-inducible enhancers. FASEB J. 9, 899–909.
[2] Roebuck, K.A. and Finnegan, A. (1999) Regulation of intercellular adhesion molecule-1 (CD54) gene expression. J. Leukoc. Biol. 66, 876–888.
[3] Yang, Y., Jun, C.D., Liu, J.H., Zhang, R., Joachimiak, A., Springer, T.A. and Wang, J.H. (2004) Structural basis for dimerization of ICAM-1 on the cell surface. Mol. Cell 14, 269–276.
[4] Jiménez, D., Roda-Navarro, P., Springer, T.A. and Casasnovas, J.M. (2005) Contribution of N-linked glycans to the conformation and function of intercellular molecules (ICAMs). J. Biol. Chem. 280, 5854–5861.
[5] Marlin, S.D. and Springer, T.A. (1987) Purified intercellular adhesion molecule-1 (ICAM-1) is a ligand for lymphocyte function-associated antigen 1 (LFA-1). Cell 51, 813–819.
[6] Diamond, M.S., Staunton, D.E., de Fougerolles, A.R., Stacker, S.A., Garcia-Aguilar, J., Hibbs, M.L. and Springer, T.A. (1990) ICAM-1 (CD54): a counter-receptor for Mac-1 (CD11b/CD18). J. Cell Biol. 111, 3129–3139.
[7] Cook-Mills, J.M. and Deem, T.L. (2005) Active participation of endothelial cells in inflammation. J. Leukoc. Biol. 77, 487–495.
[8] Hou, J., Baichwal, V. and Cao, Z. (1994) Regulatory elements and transcription factors controlling basal and cytokine-induced expression of the gene encoding intercellular adhesion molecule-1. Proc. Natl. Acad. Sci. U.S.A. 91, 11641–11645.
[9] Jahnke, A. and Johnson, J.P. (1994) Synergistic activation of intercellular adhesion molecule 1 (ICAM-1) by TNF-α and IFN-γ is mediated by p65/p50 and p65/c-Rel and interferon-responsive factor Stat1α (p91) that can be activated by both IFN-γ and IFN-α. FEBS Lett. 354, 220–226.
[10] Karin, M. and Greten, F.R. (2005) NF-κB: linking inflammation and immunity to cancer development and progression. Nat. Rev. Immunol. 5, 749–759.
[11] Baker, R.G., Hayden, M.S. and Ghosh, S. (2011) NF-κB, inflammation, and metabolic disease. Cell Metab. 13, 11–22.
[12] Perkins, N.D. (2006) Post-translational modifications regulating the activity and function of the nuclear factor kappa B pathway. Oncogene 25, 6717–6730.
[13] Ghosh, S. and Hayden, M.S. (2008) New regulators of NF-κB in inflammation. Nat. Rev. Immunol. 8, 837–848.
[14] Hayden, M.S. and Ghosh, S. (2008) Shared principles in NF-κB signaling. Cell 132, 344–362.
[15] Bhoj, V.G. and Chen, Z.J. (2009) Ubiquitylation in innate and adaptive immunity. Nature 458, 430–437.
[16] Baud, V. and Karin, M. (2009) Is NF-κB a good target for cancer therapy? Hopes and pitfalls. Nat. Rev. Drug Discov. 8, 33–40.
[17] Gilmore, T.D. and Herscovitch, M. (2006) Inhibitors of NF-κB signaling: 785 and counting. Oncogene 25, 6887–6899.
[18] Kataoka, T. (2009) Chemical biology of inflammatory cytokine signaling. J. Antibiot. 62, 655–667.
[19] Ikeda, Y., Murakami, A. and Ohigashi, H. (2008) Ursolic acid: an anti- and pro-inflammatory triterpenoid. Mol. Nutr. Food Res. 52, 26–42.
[20] Shanmugam, M.K., Dai, X., Kumar, A.P., Tan, B.K., Sethi, G. and Bishayee, A. (2013) Ursolic acid in cancer prevention and treatment: molecular targets, pharmacokinetics and clinical studies. Biochem. Pharmacol. 85, 1579–1587.
[21] Fu, L., Zhang, S., Li, N., Wang, J., Zhao, M., Sakai, J., Hasegawa, T., Mitsui, T., Kataoka, T., Oka, S., Kiuchi, M., Hirose, K. and Ando, M. (2005) Three new triterpenes from *Nerium oleander* and biological activity of the isolated compounds. J. Nat. Prod. 68, 198–206.
[22] Zhao, M., Zhang, S., Fu, L., Li, N., Bai, J., Sakai, J., Wang, L., Tang, W., Hasegawa, T., Ogura, H., Kataoka, T., Oka, S., Kiuchi, M., Hirose, K. and Ando, M. (2006)

Taraxasterane- and ursane-type triterpenes from *Nerium oleander* and their biological activities. J. Nat. Prod. 69, 1164–1167.
[23] Shishodia, S., Majumdar, S., Banerjee, S. and Aggarwal, B.B. (2003) Ursolic acid inhibits nuclear factor-κB activation induced by carcinogenic agents through suppression of IκBα kinase and p65 phosphorylation: correlation with down-regulation of cyclooxygenase 2, matrix metalloproteinase 9, and cyclin D1. Cancer Res. 63, 4375–4383.
[24] Hsu, Y.L., Kuo, P.L. and Lin, C.C. (2004) Proliferative inhibition, cell-cycle dysregulation, and induction of apoptosis by ursolic acid in human non-small cell lung cancer A549 cells. Life Sci. 75, 2303–2316.
[25] Manu, K.A. and Kuttan, G. (2008) Ursolic acid induces apoptosis by activating p53 and caspase-3 gene expressions and suppressing NF-κB mediated activation of bcl-2 in B16F–10 melanoma cells. Int. Immunopharmacol. 8, 974–981.
[26] Huang, H.C., Huang, C.Y., Lin-Shiau, S.Y. and Lin, J.K. (2009) Ursolic acid inhibits IL-1β or TNF-α-induced C6 glioma invasion through suppressing the association ZIP/p62 with PKC-ζ and downregulating the MMP-9 expression. Mol. Carcinog. 48, 517–531.
[27] Li, Y., Xing, D., Chen, Q. and Chen, W.R. (2010) Enhancement of chemotherapeutic agent-induced apoptosis by inhibition of NF-κB using ursolic acid. Int. J. Cancer 127, 462–473.
[28] Takada, K., Nakane, T., Masuda, K. and Ishii, H. (2010) Ursolic acid and oleanolic acid, members of pentacyclic triterpenoid acids, suppress TNF-α-induced E-selectin expression by cultured umbilical vein endothelial cells. Phytomedicine 17, 1114–1119.
[29] Yokomichi, T., Morimoto, K., Oshima, N., Yamada, Y., Fu, L., Taketani, S., Ando, M. and Kataoka, T. (2011) Ursolic acid inhibits Na^+/K^+-ATPase activity and prevents TNF-α-induced gene expression by blocking amino acid transport and cellular protein synthesis. Biomolecules 1, 32–47.
[30] Wang, J., Liu, L., Qiu, H., Zhang, X., Guo, W., Chen, W., Tian, Y., Fu, L., Shi, D., Cheng, J., Huang, W. and Deng, W. (2013) Ursolic acid simultaneously targets multiple signaling pathways to suppress proliferation and induce apoptosis in colon cancer cells. PLoS One 8, e63872.
[31] Tsutsui, C., Yamada, Y., Ando, M., Toyama, D., Wu, J.L., Wang, L., Taketani, S. and Kataoka, T. (2009) Peperomins as anti-inflammatory agents that inhibit the NF-κB signaling pathway. Bioorg. Med. Chem. Lett. 19, 4084–4087.
[32] Yamada, Y., Tashiro, E., Taketani, S., Imoto, M. and Kataoka, T. (2011) Mycotrienin II, a translation inhibitor that prevents ICAM-1 expression induced by pro-inflammatory cytokines. J. Antibiot. 64, 361–366.
[33] Prescher, J.A. and Bertozzi, C.R. (2006) Chemical technologies for probing glycans. Cell 126, 851–854.
[34] Dustin, M.L., Rothlein, R., Bhan, A.K., Dinarello, C.A. and Springer, T.A. (1986) Induction by IL 1 and interferon-γ: tissue distribution, biochemistry, and function of a natural adherence molecule (ICAM-1). J. Immunol. 137, 245–254.
[35] Rajagopalan, S., Xu, Y. and Brenner, M.B. (1994) Retention of unassembled components of integral membrane proteins by calnexin. Science 263, 387–390.
[36] Nakamura, N., Rabouille, C., Watson, R., Nilsson, T., Hui, N., Slusarewicz, P., Kreis, T.E. and Warren, G. (1995) Characterization of a cis-Golgi matrix protein, GM130. J. Cell Biol. 131, 1715–1726.
[37] Elbein, A.D. (1991) Glycosidase inhibitors: inhibitors of N-linked oligosaccharide processing. FASEB J. 5, 3055–3063.
[38] Klausner, R.D., Donaldson, J.G. and Lippincott-Schwartz, J. (1992) Brefeldin A: insights into the control of membrane traffic and organelle structure. J. Cell Biol. 116, 1071–1080.
[39] Chardin, P. and McCormick, F. (1999) Brefeldin A: the advantage of being uncompetitive. Cell 97, 153–155.
[40] Yan, S.L., Huang, C.Y., Wu, S.T. and Yin, M.C. (2010) Oleanolic acid and ursolic acid induce apoptosis in four human liver cancer cell lines. Toxicol. In Vitro 24, 842–848.
[41] Schwaiger, S., Zeller, I., Pölzelbauer, P., Frotschnig, S., Laufer, G., Messner, B., Pieri, V., Stuppner, H. and Bernhard, D. (2010) Identification and pharmacological characterization of the anti-inflammatory principal of the leaves of dwarf elder (*Sambucus ebulus* L.). J. Ethnopharmacol. 133, 704–709.
[42] Huang, C.Y., Liu, C.Y., Tsai, C.W. and Yin, M.C. (2011) Inhibition of cell proliferation, invasion and migration by ursolic acid in human lung cancer cell lines. Toxicol. In Vitro 25, 1274–1280.
[43] Prasad, S., Yadav, V.R., Sung, B., Reuter, S., Kannappan, R., Deorukhkar, A., Diagaradjane, P., Wei, C., Baladandayuthapani, V., Krishnan, S., Guha, S. and Aggarwal, B.B. (2012) Ursolic acid inhibits growth and metastasis of human colorectal cancer in an orthotopic nude mouse model by targeting multiple cell signaling pathways: chemosensitization with capecitabine. Clin. Cancer Res. 18, 4942–4953.
[44] Wan, L.S., Liu, T.T., Lin, X.J., Min, Q.X. and Chen, J.C. (2013) Two new chiratane-type triterpenoids from *Swertia kouitchensis*. Molecules 18, 8518–8523.
[45] Wang, Z.W., Wang, J.S., Luo, J. and Kong, L.Y. (2013) α-Glucosidase inhibitory triterpenoids from the stem barks of *Uncaria laevigata*. Fitoterapia 90, 30–37.
[46] Scott, D.W., Dunn, T.S., Ballestas, M.E., Litovsky, S.H. and Patel, R.P. (2013) Identification of a high-mannose ICAM-1 glycoform: effects of ICAM-1 hypoglycosylation on monocyte adhesion and outside in signaling. Am. J. Physiol. Cell Physiol. 305, C228–C237.
[47] Takada, Y., Matsuo, K., Ogura, H., Bai, L., Toki, A., Wang, L., Ando, M. and Kataoka, T. (2009) Odoroside A and ouabain inhibit Na^+/K^+-ATPase and prevent NF-κB-inducible protein expression by blocking Na^+-dependent amino acid transport. Biochem. Pharmacol. 78, 1157–1166.
[48] Chen, R.J., Chung, T.Y., Li, F.Y., Yang, W.H., Jinn, T.R. and Tzen, J.T. (2010) Steroid-like compounds in Chinese medicines promote blood circulation via inhibition of Na^+/K^+-ATPase. Acta Pharmacol. Sin. 31, 696–702.
[49] Chen, R.J., Jinn, T.R., Chen, Y.C., Chung, T.Y., Yang, W.H. and Tzen, J.T. (2011) Active ingredients in Chinese medicines promoting blood circulation as Na^+/K^+-ATPase inhibitors. Acta Pharmacol. Sin. 32, 141–151.
[50] Liao, Q., Yang, W., Jia, Y., Chen, X., Gao, Q. and Bi, K. (2005) LC-MS determination and pharmacokinetic studies of ursolic acid in rat plasma after administration of the traditional Chinese medicinal preparation Lu-Ying extract. Yakugaku Zasshi 125, 509–515.
[51] Shanmugam, M.K., Ong, T.H., Kumar, A.P., Lun, C.K., Ho, P.C., Wong, P.T., Hui, K.M. and Sethi, G. (2012) Ursolic acid inhibits the initiation, progression of prostate cancer and prolongs the survival of TRAMP mice by modulating pro-inflammatory pathways. PLoS One 7, e32476.
[52] Tan, Z.R., Chen, Y., Zhou, G., Cao, S., Peng, X.D., Wang, Y.C., Peng, X.J., Zhang, W. and Zhou, H.H. (2010) LC–MS–MS quantitative determination of ursolic acid in human plasma and its application to pharmacokinetic studies. Chromatograpia 72, 1107–1113.
[53] Xia, Y., Wei, G., Si, D. and Liu, C. (2011) Quantitation of ursolic acid in human plasma by ultra performance liquid chromatography tandem mass spectrometry and its pharmacokinetic study. J. Chromatogr. B Analyt. Technol. Biomed. Life Sci. 879, 219–224.
[54] Zhu, Z., Qian, Z., Yan, Z., Wang, H. and Ying, G. (2013) A phase I pharmacokinetic study of ursolic acid nanoliposomes in health volunteers and patients with advanced solid tumors. Int. J. Nanomed. 8, 129–136.